

# Performance of $\text{In}_{0.47}\text{Ga}_{0.53}\text{As}$ metal–semiconductor–metal hybrid receiver at $1.55\ \mu\text{m}$

F. TONG, D. T. McINTURFF, Y. H. KWARK, S. E. RALPH,  
G. D. PETTIT

*IBM Research Division, P.O. Box 704, Yorktown Heights, NY 10598, USA*

P. C. WONG

*Department of Information Engineering, The Chinese University of Hong Kong, Shatin, Hong Kong*

*Received 26 January; accepted 17 May 1993*

---

We report on the performance at  $1.55\ \mu\text{m}$  of a hybrid receiver combining an  $\text{In}_{0.47}\text{Ga}_{0.53}\text{As}$  metal–semiconductor–metal photodetector (with buried  $\text{AlInAs}$  buffer layer) with a  $\text{GaAs}$  MESFET preamplifier. A bit error rate of  $10^{-9}$  is measured at 1 Gbps with nonreturn to zero pseudorandom bit sequence ( $2^{15} - 1$ ) at a received optical power of  $-19\ \text{dBm}$ . Modification of the preamplifier design and a reduction of bond pad size could improve the sensitivity by  $\sim 6\text{--}7\ \text{dB}$ .

---

Metal–semiconductor–metal (MSM) photodetectors promise to be important components for systems in optical interconnect and optical networking owing to their ease of fabrication and simplified packaging through O/E integration.  $\text{InGaAs}$  MSM photodetectors with a buried  $\text{AlInAs}$  buffer layer have been grown, fabricated and characterized at  $1.3\ \mu\text{m}$  [1]. It is shown that the presence of this buffer layer dramatically reduces the parasitic capacitance, enhances carrier collection and, more importantly, effectively eliminates low-frequency gain, which is a common problem associated with MSM photodetectors. Here, we report the performance at  $1.55\ \mu\text{m}$  of a hybrid receiver combining the MSM photodetector with a  $\text{GaAs}$  MESFET preamplifier. Device characteristics of the MSM detector at  $1.55\ \mu\text{m}$  will also be discussed.

Details of the structure, MBE growth and fabrication of the  $\text{InGaAs}$  photodetector are given in [1]. Briefly, a  $1\ \mu\text{m}$   $\text{In}_{0.53}\text{Ga}_{0.47}\text{As}$  active layer is grown on top of a semi-insulating  $\text{InP}$  substrate (inset in Fig. 1). The structure includes a buried  $\text{AlInAs}$  layer to reduce the capacitance at the substrate– $\text{InGaAs}$  interface and to enhance the carrier collection. There is also a graded  $\text{InAlAs}$  top Schottky contact layer to reduce the dark current. The area between the fingers is covered with an  $\text{SiN}_x$  antireflection coating optimized for low reflection loss at  $1.3\ \mu\text{m}$ . A typical device used in this study is  $150\ \mu\text{m}$  in diameter ( $D$ ) and has an approximate finger width ( $w$ ) of  $1.5\ \mu\text{m}$  and spacing ( $s$ ) between fingers of  $2.5\ \mu\text{m}$ , resulting in 38% shadowing. Figure 1 shows the DC responsivity as a function of spectral range of the MSM detector at 300 K and 77 K. In the experiment, light from a quartz lamp was

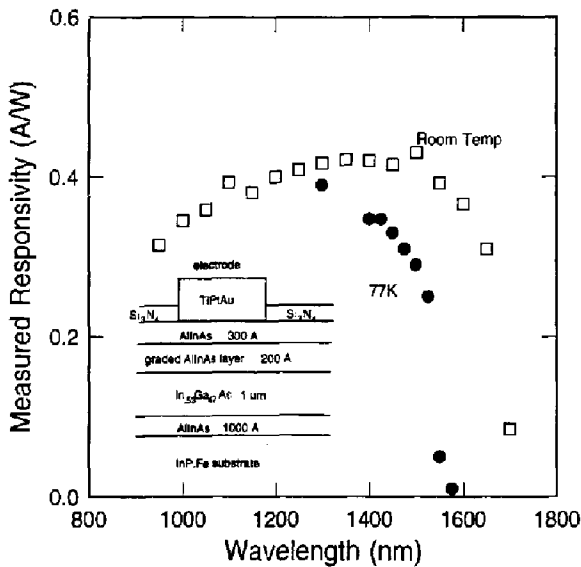


Figure 1 Responsivity versus wavelength at  $T = 300\text{ K}$  and at  $T = 77\text{ K}$  ( $D = 150\ \mu\text{m}$ ,  $s = 2.5\ \mu\text{m}$ ,  $w = 1.5\ \mu\text{m}$  and  $V = 5\text{ V}$ ) Schematic of MBE-grown InGaAs MSM photodetector is shown in the inset.

focused onto a  $\frac{1}{4}$ -m spectrometer with 2-mm slits, giving a spectral resolution of  $160\ \text{\AA}$ . A spectral filter was positioned at the spectrometer exit slit to eliminate shorter wavelengths resulting from higher diffraction orders. The light was then directed into a 20:1 microscope objective that focused the light into a  $50\text{-}\mu\text{m}$  core multimode fibre optic cable. The end of the cable was butt-coupled to the MSM detector. The light power versus wavelength was measured with an optical power meter and was of the order of  $80\text{ nW}$  for the entire wavelength range. At  $300\text{ K}$  and bias voltage,  $V$ , of  $5\text{ V}$ , the responsivity extends beyond  $1.60\ \mu\text{m}$ , while at  $77\text{ K}$  the cutoff is at  $1.5\ \mu\text{m}$ . The responsivity is nearly flat from  $1.2$  out to  $1.6\ \mu\text{m}$  and then drops off to nearly zero by  $1.7\ \mu\text{m}$ . Taking into account the 38% finger coverage, we obtain an intrinsic responsivity of about  $0.64\ \text{A W}^{-1}$  at  $1.55\ \mu\text{m}$ . We calculate that an AR coating optimized for the  $1.55\ \mu\text{m}$  range would result in about 5% improvement. We also note that the dark current at  $77\text{ K}$  and  $5\text{ V}$  is only  $550\text{ pA}$ , while at  $300\text{ K}$ , the dark current is about  $41\text{ nA}$ .

Figure 2 shows the DC response versus optical intensity of the detectors at  $1.553\ \mu\text{m}$ . As was reported earlier at  $1.3\ \mu\text{m}$ , there is early saturation of the response at  $< 1\text{ V}$ . This is an indication that the layer is depleted and that it does not suffer from an internal gain mechanism or charge pile-up at the Schottky barrier interface. After saturation, we observe a linear photoresponse versus illumination intensity. We note that the device performance showed some variation across the wafer, particularly in regard to carrier collection efficiency, resulting in some pronounced increases in responsivity with voltage. We believe that this can be minimized in future devices with improved processing and is not a problem with the device structure. The pulse response of the devices (inset in Fig. 2) was obtained using a gain-switched  $1.553\text{-}\mu\text{m}$  laser with an FWHM of  $46\text{ ps}$ . The gain-switched pulses were generated by biasing a high-speed distributed feedback laser diode (bandwidth  $\approx 6\text{ GHz}$ ) with a DC current and electrical pulses (FWHM  $\approx 57\text{ ps}$ ). The electrical pulses were generated by passing a sine wave through a

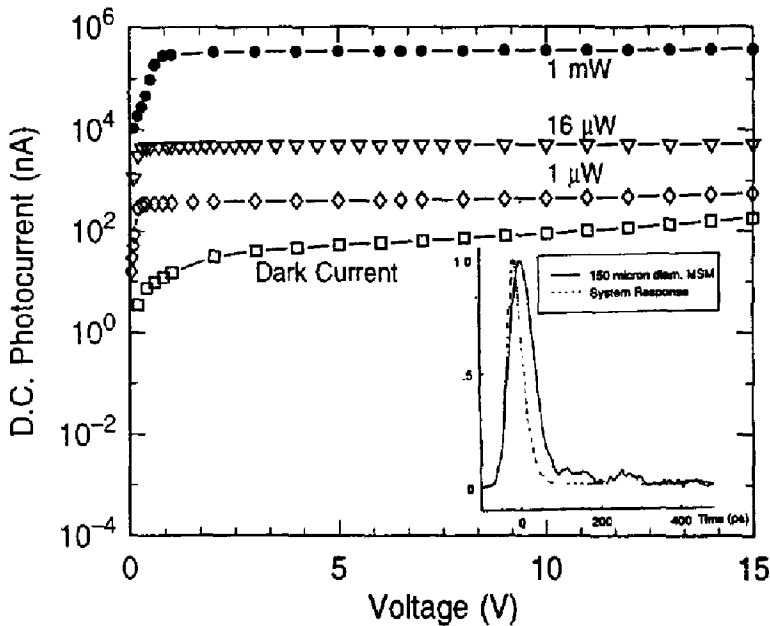


Figure 2 DC responsivity versus optical power ( $D = 150 \mu\text{m}$ ,  $s = 2.5 \mu\text{m}$ ,  $w = 1.5 \mu\text{m}$ ). Dark current is not subtracted from light response curves. The inset shows the plot of nondeconvolved pulse response of  $150 \mu\text{m}$  diameter MSM detector at 9 V (solid trace). The fall time indicates a bandwidth of  $\approx 6 \text{ GHz}$ . The laser pulse response is also shown (dashed trace).

step-recovery diode. The device pads were contacted with a 26-GHz microwave probe. The single-mode fibre was butt-coupled to the device and the response was optimized with a micromanipulator. Measurement of the fall time indicates a bandwidth of  $\sim 6 \text{ GHz}$ . No tail was observed in this response, indicating that low-frequency gain, a common problem with these devices, was not present. For all of the devices observed, the pulse width changed only slightly with bias down to 2 V, although the high-frequency responsivity decreased rapidly once the voltage was reduced below 5 V. The detector capacitance is dominated by the pad capacitance (pad dimension of  $200 \mu\text{m}$ ) of  $\sim 200 \text{ fF}$  [1] and can be reduced by reducing the pad size. The capacitance from the detector with the correction for the pad capacitance is about 35 fF for  $D = 50 \mu\text{m}$  and 185 fF for  $D = 120 \mu\text{m}$  [2].

The transimpedance amplifier utilizes a  $1\text{-}\mu\text{m}$  gate length GaAs MESFET technology with a transconductance  $g_m$  of  $150 \text{ mS mm}^{-1}$ , an  $f_T$  of 15 GHz and combined  $C_{gs}$  (gate-source capacitance) and  $C_{gd}$  (gate-drain capacitance) of 500 fF. Figure 3 shows the circuit schematically. The feedback resistance at each differential arm is  $1.5 \text{ K}\Omega$ . In the experiment, one of the differential outputs is terminated with a  $50\text{-}\Omega$  load while the other is connected to a postamplifier with a rise time of 70 ps. A 5.9-V operational voltage is applied to the MSM detector through a 7.4 V biasing to the preamplifier.

Figure 4 shows the sensitivity plot of the hybrid receiver at a transmission rate of 1 Gbps using a  $2^{15} - 1$  nonreturn to zero pseudorandom bit sequence. The receiver exhibited a sensitivity of  $-19 \text{ dBm}$  at  $10^{-9}$  bit error rate. The extinction ratio of the input signal is

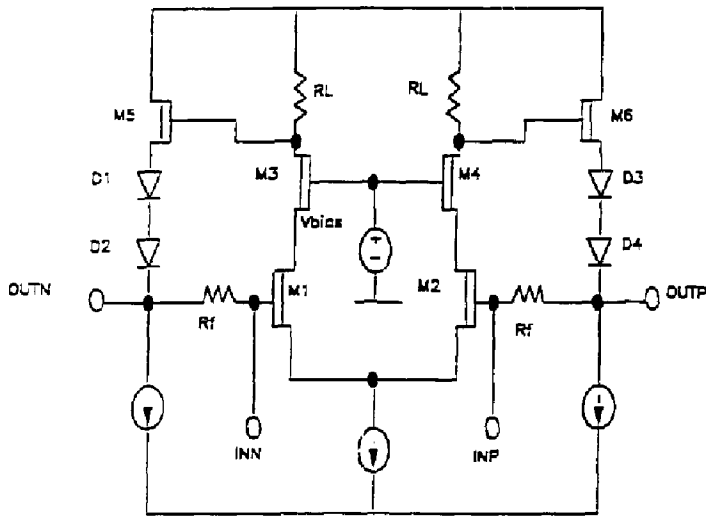


Figure 3 Circuit schematic of the differential transimpedance amplifier.

measured to be 21 dB. The performance fits well with that obtained from the theoretical values (broken line in Fig. 4) given by [3]

$$S/N = \frac{(AP)^2}{\frac{4kTI_2B}{R_L} + \frac{4kT\Gamma(2\pi C_T)^2 f_c I_1 B^2}{g_m} + \frac{4kT\Gamma(2\pi C_T)^2 I_3 B^3}{g_m} + 2qI_d I_2 B}$$

Within the approximation, the noise power of a differential preamplifier can be modelled

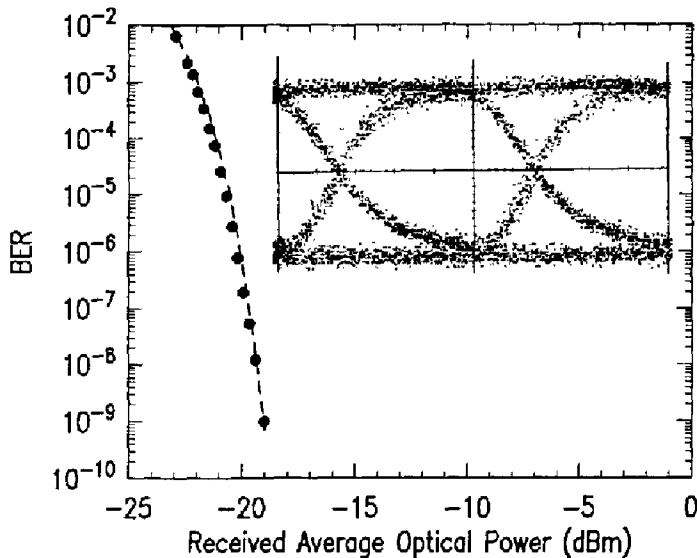


Figure 4 Sensitivity as a function of received optical power at 1 Gbps ( $D = 50 \mu\text{m}$ ,  $s = 2 \mu\text{m}$ ,  $w = 2 \mu\text{m}$ ). The measured values are represented as solid circles; the calculated values are represented by the broken line. The eye-diagram at 1 Gbps is shown in the inset.

by a single-ended preamplifier, provided the thermal noise power is contributed from both differential arms. In the above expression,  $P$  is the average incident optical power onto the detector,  $\mathcal{R}$  is the detector responsivity,  $I_2, I_3, I_f$  are normalized noise-bandwidth integrals,  $C_T$  is the total capacitance,  $k$  is the Boltzmann constant,  $B$  is the bit rate,  $q$  is the electronic charge,  $T$  is the temperature, and  $I_d$  is the detector dark current. The eye-diagram of the hybrid receiver is shown in the inset. Observation of the eye-diagram reveals that there is no additional signal level between the ONE and ZERO bit level, indicating the absence of low-frequency gain, as discussed previously. The preamplifier used was not designed for low-capacitance photodetectors; lower  $R_f$  and higher  $C$  compromise sensitivity. Modification of the amplifier can improve the performance by 5–6 dB while a reduction of pad capacitance by a factor of 2 can improve the performance by an additional  $\sim 1$  dB.

### **Acknowledgements**

The authors are grateful to D. L. Rogers and C. S. Li for many useful discussions, and to J. M. Woodall and P. E. Green for encouragement and support.

### **References**

1. S. E. RALPH, M. HARGIS and G. D. PETIT, *Appl. Phys. Lett.* **61**(18) (1992) 2222.
2. D. L. ROGERS, private communication.
3. B. L. KASPER, Receiver design, *Optical Fiber Telecommunications II* (Academic Press, New York, 1988).